

Where surface physics and fluid dynamics meet: Rupture of an amphiphile layer by fluid flow

M. M. Bandi and W. I. Goldberg^{a)}

Department of Physics and Astronomy, University of Pittsburgh, Pittsburgh, Pennsylvania 15260

J. R. Cressman, Jr.

Krasnow Institute, George Mason University, Fairfax, Virginia 22030

H. Kellay

Centre de Physique Moléculaire Optique et Hertzienne (UMR 5798), Université Bordeaux I, 351 cours de la Libération, 33405 Talence Cedex, France

(Received 12 January 2006; accepted 2 February 2006; published online 10 March 2006)

We investigate the fluctuating pattern created by a jet of fluid impinging upon an amphiphile-covered surface. This microscopically thin layer is initially covered with 50 μm floating particles so that the layer can be visualized. A vertical jet of water located below the surface and directed upward drives a hole in this layer. The hole is particle-free and is surrounded by the particle-laden amphiphile region. The jet ruptures the amphiphile layer creating a particle-free region that is surrounded by the particle-covered surface. The aim of the experiment is to understand the (fluctuating) shape of the ramified interface between the particle-laden and particle-free regions. © 2006 American Institute of Physics. [DOI: [10.1063/1.2180769](https://doi.org/10.1063/1.2180769)]

I. INTRODUCTION

It is now well known that a monatomic layer of amphiphiles on the surface of a fluid such as water can exist in several phases.^{1,2} Our understanding of the properties of these phases owes so much to the work of our dear friend Knobler and his associates. This field of surface science is but one of the many on which Professor Knobler has left an indelible mark. One of us (Goldberg) had the good fortune to be a participant in one of these adventures. The work presented here concerns his interest in surface physics and issues of fluid dynamics.

This experiment concerns the behavior of particles that float on a tank of water. The basic idea can be captured by considering what happens when one stirs a spoon of powdered cream into a cup of coffee. Assume first that the cream particles are neutrally buoyant. Stirring will quickly disperse them through the coffee. Once the process is complete, further stirring will have no apparent effect.

Now consider a variant of that experiment in which the cream particles have a density considerably less than that of water, assuring that they will stay at the air-water interface. Thus they experience a constraint not shared by the water molecules below. Stirring will induce the water molecules to come to the surface and to go back into the bulk, but the floaters are trapped on the surface.

Figure 1 shows the behavior of an initially uniform distribution of floaters in a steadily stirred fluid. Here the particles are introduced on the surface of a large tank (lateral dimensions of $1 \times 1 \text{ m}^2$) at time $t=0$. Well before then, the stirring of the tank of water has been initiated, and the fluid has reached a turbulent steady state. The motion of the par-

ticles appearing in white in Fig. 1 is captured by a high speed camera looking down on the tank from above. The stirring is vigorous (Taylor microscale $\text{Re}_\lambda \approx 150$).³ One can deduce the velocity of each particle from the recorded images.⁴ Because the particle distribution is uniform at $t=0$, an image of the particle positions at that time would be seen as a uniformly white square and hence is not shown. The camera's field of view is limited to a square of dimensions $9.3 \times 9.3 \text{ cm}^2$.

The images show that the surface particles are coagulating, not as spots but rather as linelike structures. It is seen that the coagulation is completed in roughly 1 s. A snapshot taken after several seconds would be a completely black field. This is because the particles have left the region of observation and soon reach the walls of the Plexiglass tank, where they stick.

For a discussion of the technique for studying this coagulation see Ref. 4. This reference contains details of the experiments and also simulations of the phenomenon by Schumacher *et al.* Those simulations show clearly this same coagulation phenomenon. They also demonstrate that the two dynamical Lyapunov exponents characterizing the distribution of the surface particles⁵ have opposite signs. Where they are both negative, the particles would gather into pointlike structures rather than stringlike patterns.⁶

Crucial to understanding this clustering effect of the floaters is a recognition that water is incompressible throughout the fluid volume, including all points x, y at the surface $z=0$. Thus

$$\partial_x v_x(x, y, 0, t) + \partial_y v_y(x, y, 0, t) = -\partial_z v_z(x, y, 0, t) \neq 0.$$

As the floating particles exist in two dimensions, their motion is described by the left side of this equation and hence form a compressible system. The floaters behave very differently than the water molecules on which they move. Water

^{a)}Electronic mail: goldburg@pitt.edu

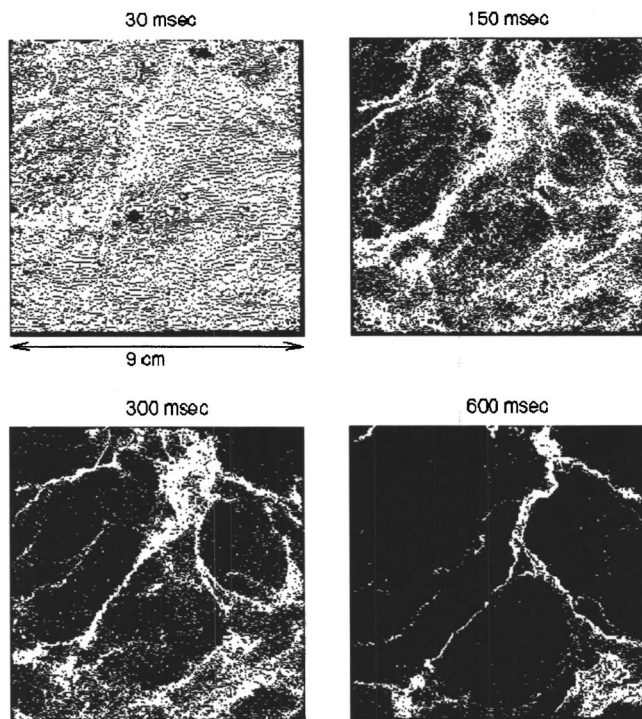


FIG. 1. Evolution of particle density of floaters that are initially distributed uniformly at $t=0$. Tracers appear in white. For these measurements, $Re_\lambda = 140$, $\lambda = 0.4$ cm, integral scale, and $l_0 = 3.8$ cm.

molecules at the surface can acquire vertical components of velocity $v_z(x, y, 0, t)$ whereas the floaters cannot. By virtue of their buoyancy, the motion of floaters is governed by the left side of this equation, assuring for them that $\partial_x v_x(x, y, 0, t) + \partial_y v_y(x, y, 0, t) \neq 0$.

One may argue that because the surface is not perfectly flat, the floaters participate in three-dimensional motion by virtue of the presence of capillary waves.^{7,8} This effect is small, however, as was established by ancillary experiments.⁹ One can define a dimensionless compressibility C that ranges from zero to unity if the turbulence is isotropic. Measurements and computer simulations establish that $C \approx 0.5$.^{4,6}

It is at this point in the story that surface physics enters. The clustering that is so apparent in Fig. 1 is absent if the surface is covered with an amphiphile layer. Therefore, the surface must be freshly “vacuumed” or “skimmed” before images such as those in Fig. 1 are made.⁴ Typically, the “surface vacuum cleaning” is initiated well before the camera is switched on and continues throughout the duration of the experiment. The skimmers are placed far from the region of observation for the surface turbulence experiments.

II. EXPERIMENT

The present experiments are aimed at understanding the role of the contaminating amphiphile layer in influencing the distribution of particles on the surface. Here an amphiphile layer is deliberately placed on the surface of a smaller tank of water (lateral dimensions of 20×30 cm²). This layer is ruptured by a jet of water coming from inside the tank and directed upward toward the surface (see Fig. 2). Water from

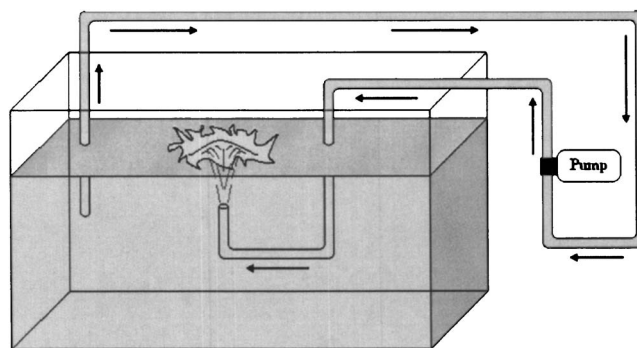


FIG. 2. A sketch of the experimental setup. The tank has lateral dimensions of 20×30 cm² and is filled with water to a height of about 30 cm. The jet is placed 10 cm below the surface. An amphiphile monolayer is introduced on the surface prior to the experiment. A micropump circulates water from the tank through the jet rupturing the monolayer. Particles constantly seeded onto the surface from the jet allow visualization of the ruptured interface between the water and amphiphilic monolayer.

the tank is fed into a small pump that supplies the vertical jet. The orifice of the jet, located 10 cm below the surface of the water, has a diameter of 1 cm. Because the output of the jet and its input are both inside the tank, the water level remains constant. The flow rate from the jet is small enough so as to produce only a slight bulge (~ 2 mm) at the water surface directly above it. The diameter of the bulge is a few centimeters.

When the jet’s vertical output hits the surface it is diverted radially outward, its maximum speed near the center being of the order of 35 cm/s (see Fig. 3). The field of view here is about 5×5 cm². In this figure local velocities are represented by the length and direction of the small arrows. Near the center of the jet the arrows are very short, signifying that the flow is mainly upward.

It is clear that the flow is not strongly turbulent, as it is in

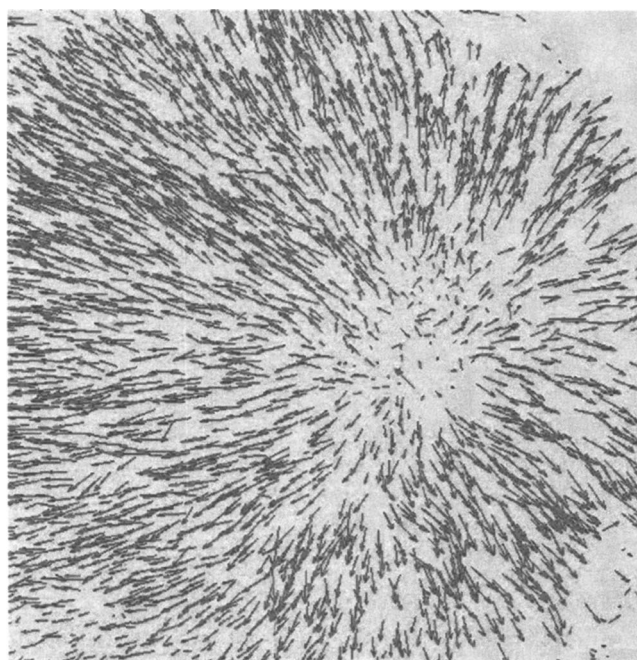


FIG. 3. Velocity vector field of the radial flow at the surface as measured by particle imaging velocimetry Ref. 4. The field of view is 5×5 cm².

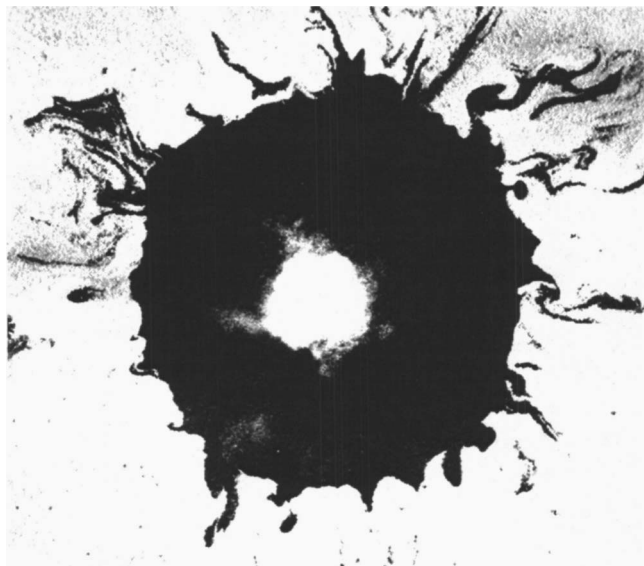


FIG. 4. A snapshot showing the ramification of the amphiphilic monolayer at the air-water interface. In the steady state this pattern fluctuates in time, but the mean diameter of the dark annulus remains roughly constant. The tentacles change in depth, orientation, and shape. Their typical length is of the order of $a=1$ cm.

Fig. 1. Near the edge of the image there are very few velocity vectors. This is because the surface there is so densely covered with particles that their individual positions and velocities become immeasurable.

Figure 4 is a photo made by the overhead fast camera. The lateral dimensions of the image are about 10×10 cm². Prior to the measurement, the surface of the water is covered with a layer of fatty acid (oleic acid) at close packing density of roughly $20 \text{ \AA}^2/\text{molecule}$. The amphiphile layer is expected to be in a condensed phase.^{1,2,10} The white region in the center of the image is an in-plane view of the jet at the surface. It appears to be white because a high concentration of 50 \mu m particles is being steadily injected by the jet into the tank. The particles spend very little time upon reaching the surface and are quickly swept away towards the ring. The black region is therefore free of particles. Either all of the black region or an inner circle (of diameter somewhat larger than the inner white region) is likewise free of the amphiphile layer. The particles are hollow glass spheres that show no sign of interaction with each other. Surface tension will favor coagulation of particles, but this effect is small compared to forcing effect of the jet.

III. DISCUSSION

The central problem posed by Fig. 4 is that of explaining the origin of the irregularly shaped arms or tentacles that extend into the white area. It is believed that these particles densely cover the amphiphile layer, which is of molecular thickness and hence is not visible. The average diameter of the particle-free region is about 10 cm. It is not certain if the particle-free region in the dark annulus is truly amphiphile-free.

A movie shows that the tentacles, as well as the diameter of the annulus, fluctuate in shape from one moment to the next, with a correlation time of the order of a fraction of a

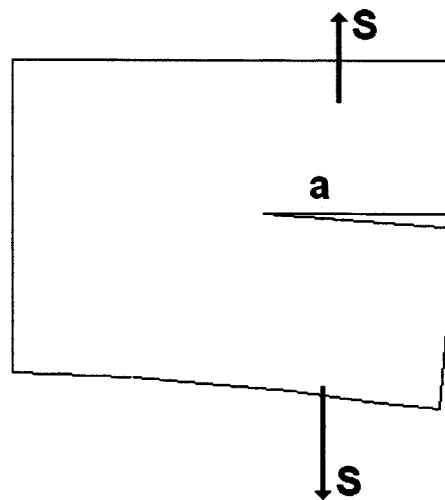


FIG. 5. Type I fracture of a three-dimensional solid. For a given stress S , the crack length a will spontaneously grow if S exceeds a critical value S_c , where S_c depends upon the Young's modulus of the solid and the surface energy increase that comes from creating the crack. If S is set to a particular value, a crack of length a will spontaneously grow only if a exceeds some critical value $a=a_c$. If $a < a_c$, the crack heals.

second. If the jet is suddenly switched off, the dark annulus collapses and the surface becomes uniformly covered with the surfactant. Presumably this tendency to uniform coverage corresponds to a lowering of the surface energy of the system. Careful observation of the collapse suggests that the amphiphile layer is moving inward so fast that the macroscopic floating particles become detached from this microscopic layer. As a result, radial black particle-free streaks remain for many minutes after the (particle-free) annulus has been filled in.

So far no compelling explanation has emerged that can account for the shape of the ramified pattern shown in Fig. 4. The image suggests that perhaps outward flow from the jet creates a temporally fluctuating shear that breaks the amphiphile layer and that the floating particles sit on that microscopically thin layer, making it observable. If so, the flow-generated temporarily fluctuating stress may be playing a role similar to that of the static stress in the theory of fracture of a solid.¹¹⁻¹⁴

Decades ago Griffith¹⁵ advanced a simple energy argument to explain how a fracture develops. The mechanism is illustrated in Fig. 5. Shown there is a solid that extends into the page at a distance w . The solid is assumed to be homogeneous and to be characterized by the three-dimensional version of Hooke's law (stress proportional to strain). In the type of fracture considered here, and called a type I fracture, a cut of length a is made into a solid and the two exposed surfaces are pried apart with a stress S .

The elastic energy of the system is reduced by the lengthening of the crack but there is a surface energy cost that opposes this. A one-dimensional analogy is that of the stretching of a spring by a mass m on its end. Though it costs energy $\Delta E_1 = \frac{1}{2}ka^2$ to stretch the spring of spring constant k , there is a decrease in gravitational energy $\Delta E_2 = -mga$ of the mass attached to it. Since $mg=ka$, $\Delta E_2 = -ka^2$. Therefore the

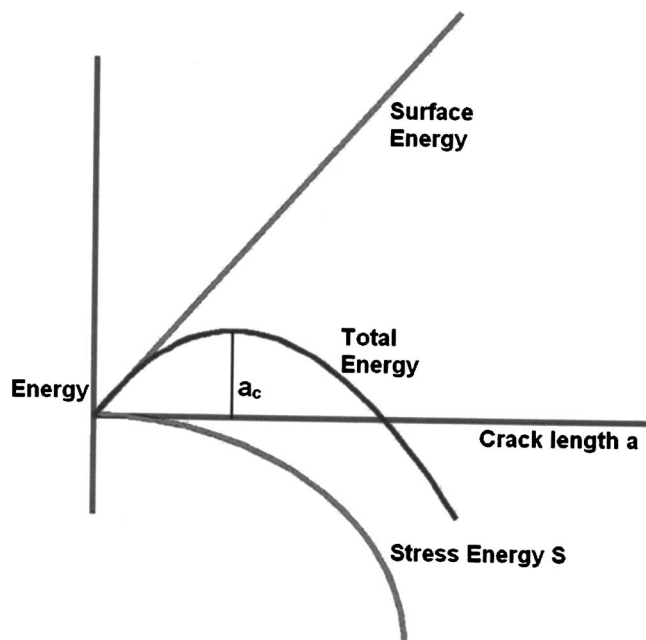


FIG. 6. Type I fracture of a three-dimensional solid. For a given stress S , the crack length a will spontaneously grow if S exceeds a critical value S_c , where S_c depends upon the Young's modulus of the solid and the surface energy increase that comes from creating the crack. If S is set to a particular value, a crack of length a will spontaneously grow only if a exceeds some critical value $a = a_c$. If $a < a_c$, the crack heals.

total energy change is $\Delta E_b = \Delta E_1 + \Delta E_2 = -\frac{1}{2}ka^2$, a negative quantity. In both one dimension (1D) and two dimensions (2D), the energy decrease is proportional to a^2 if the solid obeys Hooke's law. However, as the crack grows, there is a positive contribution $2\gamma aw$, where γ is a surface energy coefficient, or surface tension (the crack has two faces, hence the factor of 2). Figure 6 shows the energy contributions of the two terms in the Griffith theory. Beyond a critical length a_c , a crack will spontaneously grow; for smaller lengths it will heal. At $a = a_c$ the system is in a state of unstable equilibrium.

For the brittle fracture of a three-dimensional (3D) solid of Young's modulus E , the stress σ_c required to make a crack of length a marginally unstable to spontaneous growth is given by

$$\sigma = A\sqrt{E\gamma/a},$$

where A is a constant of order unity,¹³ E is Young's modulus (in pascals), and γ is the surface energy (in N/m) required to create a fracture. One may ask if this expression can be applied to the fracture of a 2D amphiphile layer, with E and γ replaced by their two-dimensional counterparts. Both the 2D Young's modulus E_2 of an amphiphile layer and the corresponding surface energy γ_2 have been measured, though not in oleic acid. Roughly speaking these coefficients are in the range of $E_2 \approx 20$ mN/m (in pentadodecanoic acid¹⁶) and $\gamma_2 \approx 30$ pN (in methyl-octadecanoate¹⁷). The fingers in Fig. 4 have a length of the order of 1 cm. Inserting this parameter in the above equation and using the above values of E_2 and γ_2 , one estimates a critical stress of the amphiphile layer σ_c of the order of 10^{-5} N/m.

It is assumed that the stress that ruptures the amphiphile layer originates from the radial flow. The source of the corresponding two-dimensional stress, now called σ_2 , is the viscous shear on the amphiphile covering. That stress is taken to be $\sigma_2 = (2\pi R)\eta(\Delta U/\Delta y)$, where ΔU is taken to be the difference between the radial velocity of the amphiphile layer and the flow rate near the surface when the amphiphile layer is absent. Its value is roughly $\Delta U = 10$ cm/s. This gradient is across a vertical distance Δy that has not been measured; it is estimated to be $\Delta y = 1$ cm (the jet originates at a distance of 5 cm below the surface). Taking $\eta = 0.01$ P for water and the radius of the amphiphile-free hole is $R = 5$ cm roughly give a crude estimate of the two-dimensional stress $\sigma_2 \approx 10^{-3}$ N/m, two orders of magnitude larger than $\sigma_c = 10^{-5}$ N/m. If these estimates are to be trusted, the radial shear on the amphiphile layer is more than sufficient to create fissures into the amphiphile-covered (and particle-covered) region in Fig. 4.

Though the fjordlike channels in Fig. 4 do not resemble fracture lines seen in solids, it has been found that a hydrophobic layer of lycopodium powder is fractured by an amphiphile introduced on it.¹⁸ It has also been suggested that the phenomenon observed in this experiment is related to the viscous fingering instability.¹⁹ It appears, however, that this explanation requires that the underlying fluid be microscopically shallow (private communication with Troian and Ref. 20), which seems to rule out viscous fingering. It is suggested above that the ramified structure observed in Fig. 4 is related to a balance between the stress applied by the jet and the one-dimensional surface energy of the amphiphile layer. The irregular structure of the intrusions may arise because the flow is chaotic rather than laminar. It must be noted that unlike the fracture in brittle solids, the tentacles observed in this experiment are initially very blunt and only later evolve into sharper tips.

IV. SUMMARY

Particles floating on the freshly cleaned surface of a tank of turbulent water coagulate in a way that is expected for a compressible fluid. However, if that surface is covered with an amphiphile layer, this coagulation effect is blocked. The experiments described here are aimed at understanding the role of this layer in a fluid dynamics setting. That layer is rendered visible by a covering of small particles that float on the water's surface. It comes as no surprise that the jet will break a hole in the particle covering. If the surface is amphiphile-free, that hole is smooth and expands to the edge of the tank. On the other hand, if the amphiphile covering is present, this hole develops irregularly shaped tendrils at its rim and these particle-free regions fluctuate in space and time. An admittedly crude argument suggests that the observed phenomenon may be understood in terms of the theory of fracture. Only further and more extensive experiments will determine if the fracture approach has merit. In any case, the observed patterns are intriguing and call for an explanation.

ACKNOWLEDGMENTS

This work was supported by the National Science Foundation Grant DMR No. 0201805. The authors have benefited greatly from the discussions with C. M. Knobler, Thomas Fischer, Sandra Troian, and the University of Pittsburgh Softmatter group. The authors also acknowledge Michael Turner for help with initial measurements.

¹V. M. Kaganer and P. Dutta, *Rev. Mod. Phys.* **71**, 779 (1999).

²C. M. Knobler, *J. Phys.: Condens. Matter* **3**, S17 (1991).

³U. Frisch, *Turbulence: The Legacy of A. N. Kolmogorov* (Cambridge University Press, Cambridge, 1995).

⁴J. R. Cressman, J. Davoudi, W. I. Goldburg, and J. Schumacher, *New J. Phys.* **6**, 53 (2004).

⁵R. C. Hilborn, *Chaos and Nonlinear Dynamics: An Introduction for Scientists and Engineers* (Oxford University Press, New York, 1994), p. 1.

⁶G. Boffetta, J. Davoudi, B. Eckhardt, and J. Schumacher, *Phys. Rev. Lett.* **93**, 134501 (2004).

⁷V. E. Zakharov, V. L'vov, and G. Falkovich, *Kolmogorov Spectra of Turbulence I: Wave Turbulence*, Springer Series in Nonlinear Dynamics

(Springer-Verlag, New York, 1992).

⁸W. I. Goldburg, J. R. Cressman, Z. Vörös, B. Eckhardt, and J. Schumacher, *Phys. Rev. E* **63**, 065303 (2001).

⁹E. Schröder, J. S. Andersen, M. T. Levinsen, P. Alström, and W. I. Goldburg, *Phys. Rev. Lett.* **76**, 4717 (1996).

¹⁰C. M. Knobler, *Adv. Chem. Phys.* **77**, 397 (1990).

¹¹L. B. Freund, *Dynamic Fracture Mechanics* (Cambridge Monographs on Mechanics, 1998).

¹²D. Bonn, H. Kellay, M. Prochnow, K. Ben-Djemaa, and J. Meunier, *Science* **280**, 265 (1998).

¹³J. Fineberg and M. Marder, *Phys. Rep.* **313**, 1 (1999).

¹⁴J. F. Knott, *Fundamentals of Fracture Mechanics* (Butterworth, Washington, DC, 1973).

¹⁵A. A. Griffith, *Philos. Trans. R. Soc. London, Ser. A* **221**, 163 (1920).

¹⁶E. Hatta and T. M. Fischer, *Langmuir* **18**, 6201 (2002).

¹⁷S. Wurlitzer, P. Steffen, M. Wurlitzer, Z. Khattari, and T. M. Fischer, *J. Chem. Phys.* **113**, 3822 (2000).

¹⁸D. Vella, P. Aussillours, and L. Mahadevan, *Europhys. Lett.* **68**, 212 (2004).

¹⁹P. G. Saffman and G. I. Taylor, *Proc. R. Soc. London, Ser. A* **245**, 312 (1958).

²⁰S. M. Troian, E. Herbolzheimer, and S. A. Safran, *Phys. Rev. Lett.* **65**, 333 (1990).

The Journal of Chemical Physics is copyrighted by the American Institute of Physics (AIP). Redistribution of journal material is subject to the AIP online journal license and/or AIP copyright. For more information, see <http://ojps.aip.org/jcpo/jcpcr/jsp>